ANALYSIS OF INSTALLATION FORCES FOR HELICAL PILES IN CLAY

J. P. Hambleton[1], S. A. Stanier[2], C. Gaudin[2], K. Todeshkejoei[1]
[1]*ARC Centre of Excellence for Geotechnical Science and Engineering, The University of Newcastle, Callaghan, NSW, Australia*
[2]*ARC Centre of Excellence for Geotechnical Science and Engineering, The University of Western Australia, Crawley, WA, Australia*

ABSTRACT

Installation forces play a central role in the design and performance of helical piles, especially since the installation torque is often used as an indicator of the pile's ultimate capacity. This paper presents an analytical model for predicting the installation torque for single-helix piles in clay. As an extension of a recent study by the authors, the proposed model considers not only the forces occurring on the helical plates but also the shear stresses generated along the shaft, both of which impact the installation forces. The model yields a straightforward expression that relates installation torque to the undrained shear strength of the soil, embedment depth, helix diameter and pitch, shaft diameter, crowd (axial) force, and adhesion coefficient along the shaft. The influence of these factors on the installation torque, as well as the "capacity-to-torque ratio" used to infer capacity from the installation, is assessed through a sensitivity analysis. Some level of validation is provided through a comparison with empirical capacity-to-torque ratios, and the sensitivity analysis reveals factors that are neglected in empirical models but nevertheless have a significant influence.

1 INTRODUCTION

Helical piles are deep foundations consisting of one or more helical plates mounted to a central shaft. Their main feature is the method of installation, which involves twisting the pile into the ground under an applied torque and crowd (axial) force. On account of the relative ease of the installation process compared to traditional deep foundations (e.g., driven and drilled piles) and growing acceptance within the geotechnical engineering community, the popularity of helical piles has risen markedly over the past few decades. Figure 1 depicts several applications where helical piles are routinely used. Apart from these well-established applications, helical anchors have been identified as a promising foundation solution for near-shore wave energy converters. Common alternatives to the term "helical pile" include "screw piles" and "helical anchors," the latter being reserved for applications involving uplift (e.g., Figures 1b, 1c, and 1d).

As with most types of foundation, the vast majority of the theory developed for helical piles focuses on the uplift or bearing capacity of the configuration at its final embedment depth, without regard for the process of installation. The rigorous analyses conducted by Merifield (2011) and Wang *et al*. (2013), discussed further in the companion paper in this issue (Gaudin *et al*., 2014) are examples where such "wished-in-place" conditions are assumed. The monograph by Perko (2009) provides a complete overview of the prevailing methods for predicting uplift and bearing capacity of helical piles alongside a summary of their historical development, design issues, example applications, practical aspects of installation, field testing and loading conditions.

Despite the recognised impacts of the installation process on the performance of helical piles (cf. Perko 2009; Tsuha *et al*., 2012), and in particular the widely adopted use of installation torque as an indicator of ultimate capacity, relatively few attempts have been made to model the installation process theoretically. This can be attributed to the degree of difficulty, since the installation process involves large, predominantly plastic deformation, contact interaction at the soil-helix and soil-shaft interfaces, and material separation at the leading edge of the helical plates as they cut the soil. Ghaly *et al*. (1991) and Tsuha and Aoki (2010) proposed analytical models for predicting the installation torque for helical piles in sand, and Perko (2000) developed an approximate model that directly relates the bearing or uplift capacity to the installation torque via balance of energy. Whereas the former models pertain specifically to sand, an acknowledged peculiarity of Perko's model is the absence of soil strength parameters. Perko's model is nevertheless consistent with previously established empirical models that relate the bearing or uplift capacity to the installation torque without consideration for the material type. In particular, the widely accepted method referred to here as "torque-capacity correlation" relies on the following empirical formula (Hoyt and Clemence, 1989)

$$F_{\max} = KT \tag{1}$$

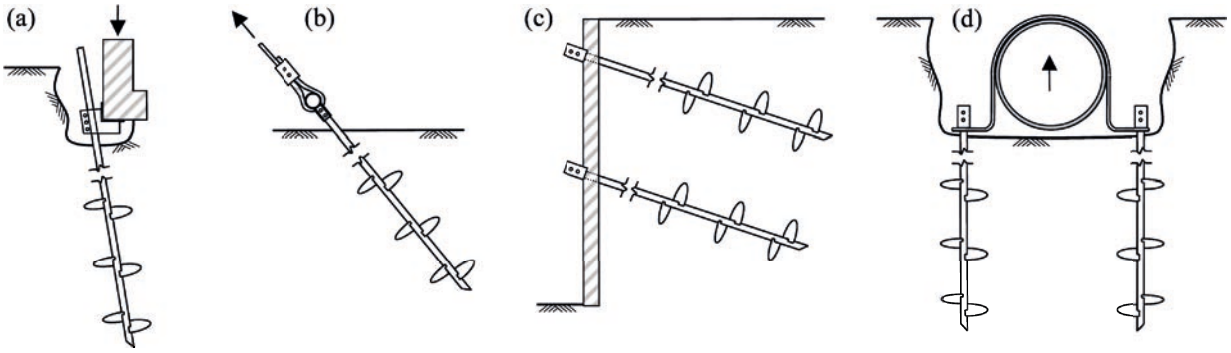

Figure 1: Conventional applications for helical anchors: (a) foundation underpinning, (b) guy wire anchors, (c) tiebacks for retaining walls, and (d) buoyancy control for pipelines.

where F_{max} is the maximum force that can be sustained in uplift or compression, K is a constant known as the "capacity-to-torque ratio," and T is the installation torque measured at the final embedment depth. The ratio K is usually regarded as depending only on the diameter of the shaft, denoted by d. Accordingly, Perko (2009) proposed the following expression

$$K = 1433 d^{-0.92} \tag{2}$$

where K and d have units of m^{-1} and mm, respectively. Equation (2) is considered to be equally valid for sand and clay.

This paper presents a new analytical model that relates the installation forces to the pile dimensions, embedment depth, and soil shear strength for a single-helix pile in saturated clay. The model pertains to a deeply embedded pile installed relatively rapidly, so that undrained conditions apply, and it furthermore assumes a uniform strength profile with the soil characterised by a single value of undrained shear strength s_u. By incorporating the effects of shear stresses along the shaft generated through adhesion, the model extends the work of Todeshkejoei *et al*. (2014), who established yield envelopes that relate the torque on a single deeply embedded helix to the applied axial force, helix geometry, and soil shear strength. The model is based on equilibrium between the installation forces and the forces generated along the shaft and at the helix (which alone provides an insufficient number of equations to solve for the unknowns) and on kinematics of the installation process. The analysis results in a convenient formula that is subsequently used to investigate the influence of the axial force, pile geometry, and soil shear strength on the installation torque. By also considering the undrained uplift and bearing capacity F_{max}, the influence of these parameters on the capacity-to-torque ratio K is also explored. The paper concludes with a discussion regarding practical implications and future work.

2 ANALYTICAL MODEL

The model presented in this paper is for a helical pile with a circular shaft with diameter d and a single helix of diameter D and pitch p (Figure 2a). The pile is installed in a vertical orientation with a torque T and axial force N. In general, the forces T and N can vary throughout the installation process depending not only on operating conditions but also on the increase in resistance at increasing values of the embedment depth H, which from a modelling viewpoint parameterises the installation process. This study focuses on the advanced stages of the installation process for which the soil around the helical plate undergoes localised failure (cf. Merifield, 2011; Todeshkejoei *et al*., 2014).

To advance the helical pile into the soil, the installation forces T and N must overcome the resistance generated by the helical plate as it cuts through the soil and by relative sliding at the shaft-soil interface. Moreover, equilibrium requires

$$T = T_p + T_s, \quad N = N_p + N_s \tag{3}$$

where the subscripts "p" and "s" denote forces generated by the helical plate and the shaft, respectively. The analysis considers standard installation, where the forces are always directed as shown in Figure 2(b). Namely, it is assumed that N is always compressive ($N > 0$) and sufficiently large to overcome the resistance from the shaft ($N \geq N_s$). If this is not the case, the helical plate will be subjected to uplift, and the corresponding reaction on the pile will be directed downward ($N_p < 0$) in Figure 2(b). If N_s is large relative to N_P, this condition causes the pile to rotate without advancing into the soil (i.e., over-rotation or augering).

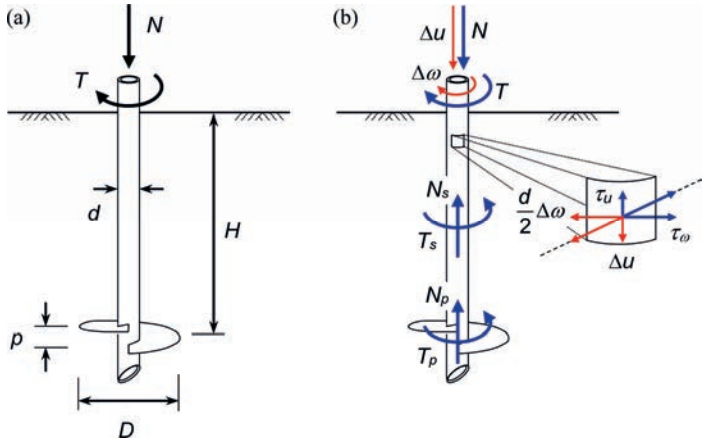

Figure 2: Schematic of a deeply embedded helical pile with a single helical plate: (a) installation forces and key dimensions; (b) forces on the shaft and helical plate and shear stresses generated along the shaft.

Based on a large number of numerical simulations, Todeshkejoei *et al*. (2014) proposed the following yield envelope relating the torque T_p to the axial (normal) force N_p for single deeply embedded helical plate

$$\left(\frac{N_p}{N_{p,\max}}\right)^q + \left(\frac{T_p}{T_{p,\max}}\right)^r = 1 \tag{4}$$

where

$$q = 1.07, \quad r = 5.16 - 8.02\frac{p}{D}, \quad N_{p,\max} = 10.82 s_u D^2 \left[1 - \left(\frac{d}{D}\right)^2\right]\left[1 + \left(\frac{p}{D}\right)^2\right]^{-\frac{1}{2}}, \quad T_{p,\max} = s_u D^3 \left[0.74 + 0.33\frac{p}{D}\right] \tag{5}$$

Equation (4) was established through small-strain finite element analyses in which a helical plate was rotated under an applied normal force N_p until the reaction torque reached the limiting value T_p. The simulations considered a true three-dimensional helical geometry with an aperture corresponding to the diameter of the shaft d, but the influence of the shaft was otherwise neglected. The relationships given in Equation (4) were determined via curve fitting and they are valid for a rough helical plate with a thickness of $t = 0.05D$, $0.16 \le p/D \le 0.48$, and $0 \le d/D \le 0.4$.

Along the shaft, the torque T_s and axial force N_s develop through relative sliding at the interface between the shaft and the soil. The conventional adhesion model for clays is assumed, where the limiting magnitude of the shear stress τ is given by $\tau = \alpha s_u$ and α is the so-called adhesion coefficient ($0 \le \alpha \le 1$). As depicted in Figure 2(b), the magnitude of the shear stress is determined by an axial component τ_u and an angular component τ_ω, where $\tau = (\tau_\omega^2 + \tau_u^2)^{1/2} = \alpha s_u$. Assuming that the shear stresses are constant along the length and perimeter of the shaft, the shaft forces are given as $N_s = \pi d H \tau_u$ and $T_s = \pi d^2 H \tau_\omega / 2$, and using the aforementioned adhesion model, these forces are related by

$$\sqrt{\left(\frac{N_s}{\pi d H}\right)^2 + 4\left(\frac{T_s}{\pi d^2 H}\right)^2} = \alpha s_u \tag{6}$$

Considering the axial force N to be a specified constant corresponding to the crowd force applied during installation, Equations (3)-(6) provide four equations for five unknowns (T, T_p, T_s, N_p, and N_s) and a fifth equation is therefore needed in order to close the system of equations.

The first key postulate utilised in this paper is that the shear stress vector with components τ_u and τ_w is parallel to the displacement vector at the shaft-soil interface, which consists of an axial component Δu and an angular component $d\Delta\omega/2$, where Δu and $\Delta\omega$ are the incremental axial displacement and rotation of the pile, respectively. This assumption, illustrated in Figure 2(b), is consistent with the concept of direct shear testing, where the mobilised resistance directly opposes the motion, and it provides the following relationship

$$\frac{\tau_\omega}{\tau_u} = \frac{2T_s}{dN_s} = \frac{d}{2}\frac{\Delta\omega}{\Delta u} \tag{7}$$

The second key postulate is that the pile advances into the soil at a rate determined by the pitch of the helical plate. In this condition, referred to as "neutral rotation," the pile advances by a displacement increment $\Delta u = p$ for one revolution of the pile, $\Delta\omega = 2\pi$. While the validity of this assumption remains to be explored in depth, it is fully consistent with standard installation procedures. For example, Perko (2009) notes that "the crowd applied should be sufficient to ensure that the helical pile advances into the ground a distance equal to at least 80 percent of the blade pitch during each revolution" and his method for predicting the capacity-to-torque ratio (Perko, 2000) rests on a similar assumption. Substituting $\Delta\omega/\Delta u = 2\pi/p$ into Equation (7) gives the following relationship between T_s and N_s.

$$\frac{T_s}{N_s} = \frac{\pi d^2}{2p} \tag{8}$$

The following formula, expressing the installation torque T in terms of the remaining variables, can be determined by solving Equations (3)-(8)

$$T = \frac{\pi^2 \alpha s_u d^3 H}{2\sqrt{p^2 + \pi^2 d^2}} + T_{p,\max} \left\{ 1 - \left[\frac{1}{N_{p,\max}} \left(N - \frac{\pi \alpha s_u dHp}{\sqrt{p^2 + \pi^2 d^2}} \right) \right]^q \right\}^{\frac{1}{r}} \tag{9}$$

where q, r, $N_{p,\max}$ and $T_{p,\max}$ are given by Equation (5). While Equation (9) is valid for any value of the adhesion coefficient α, it should be noted that the expressions for q, r, $N_{p,\max}$ and $T_{p,\max}$ given by Equation (5) correspond to $\alpha = 1$. Expressions for alternative values of α can be readily developed using an approach similar to the one described by Todeshkejoei *et al*. (2014). Throughout the remainder of this paper, a rough shaft and helical plate ($\alpha = 1$) are assumed.

Having established a formula for the installation torque T, the derivation of an expression for the capacity-to-torque ratio K in Eq. (1) simply requires an expression for the bearing or uplift (axial) capacity $F_{\max}$. In determining the axial capacity, the influence of the shaft is typically neglected (cf. Perko. 2009; Merifield, 2011; Gaudin *et al*., 2014) as a means of simplifying the calculations and arriving at a conservative estimate. This simplification is justified for small shaft-to-helix diameter ratios, as considered here ($d/D \leq 0.4$). The same approach is used for consistency, recognising that shaft resistance can be easily incorporated by superposition for larger diameter ratios. Hence, $F_{\max}$ is given by the maximum force that can be sustained by the helical plate, $F_{\max} = N_{p,\max}$, and the capacity-to-torque ratio is

$$K = \frac{N_{p,\max}}{T} \tag{10}$$

The formula for $N_{p,\max}$ given in Equation (5) compensates for the effects of the ratios d/D and p/D but overall gives values that are close to the exact solution $N_{p,\max} = 10.3 s_u D^2$ determined by Martin and Randolph (2001) for a deeply embedded circular plate (i.e., a helical pile with $d = p = 0$) assuming an infinitesimally thin plate and rough contact.

3 SENSITIVITY ANALYSIS

This section presents a sensitivity analysis to quantify the influence of the undrained shear strength s_u, embedment depth H, helix diameter D, pitch p, shaft diameter d, and axial force N on the installation torque T and torque-capacity ratio K, based on the formulae developed in the previous section. The ratio between the torques mobilised by the shaft and the helical plate, T_s/T_p, is also investigated to ascertain the influence of the shaft.

The sensitivity analysis is completed by first identifying typical values for each of the parameters and then, using that set of representative parameters as a basis, varying each parameter independently to distinguish its effect. As a typical value for a medium strength clay, $s_{u,0} = 40$ kPa was selected for the undrained shear strength. As with the remaining parameters, the subscript "0" indicates the role of the specified constant as a basis. For the dimensions of the helical pile, the database assembled by Perko (2009) can be used to ascertain the following typical (median) values: $D_0 = 250$ mm, $p_0 = 70$ mm, and $d_0 = 50$ mm. A value of $H_0 = 1.5$ m is selected for the embedment depth to achieve an embedment ratio of $H_0/D_0 = 6$, which roughly corresponds to the embedment ratio necessary for a localised failure mechanism to develop around the helical plate and, consequently, for the plate to achieve its maximum capacity (Merifield, 2011). The normal force is initially set to a value of $N_0 = 10$ kN, but given the absence of information regarding the axial forces that are typically applied during installation (cf. Perko, 2009), a range of possible values is subsequently explored.

Figure 3 plots the results of the sensitivity analysis for the selected base values and reveals that the undrained shear s_u, helix diameter D, and shaft diameter d each have a strong influence on the torque. Among these, the helix diameter has the strongest effect, with a 50% increase in the helix diameter causing an increase in the torque of well over 100% for the particular case considered. By comparison, the influence of the shaft is much smaller, with a 50% increase causing an increase in the torque of less than 50%. The embedment depth H has a relatively modest effect (as long as the embedment remains deep), and the pitch p has virtually no effect.

Figure 3 also shows that the torque mobilised along the shaft, T_s, is relatively small compared to the torque mobilised by the helical plate, T_p. For the base parameters, the ratio is $T_s/T_p \approx 45\%$, and the torque mobilised along the shaft accounts for only 31% of the total torque T. As one would expect, the contribution from the shaft grows significantly as the helix diameter D decreases and the shaft diameter d increases, as seen in Figures 3(c) and 3(f), respectively.

Figure 4 displays the influence of the various parameters on the capacity-to-torque ratio K. As illustrated by the lack of dimensional homogeneity in the empirical model of Equation (2), K cannot be interpreted on its own as a physically meaningful quantity, and therefore it is normalised by D in Figure 4, recognising that D is the parameter with the strongest influence on the torque and axial capacity. The figure also compares the predictions of KD from the proposed

model, Equation (10), with the values given by the empirical model, Equation (2). Overall, the values obtained with the two models are in reasonable agreement. For the base parameters, the proposed model predicts $KD = 9.03$ compared to $KD = 9.80$ from the empirical model, a difference of roughly 8%. Both models suggest that the capacity-to-torque ratio is relatively insensitive to the undrained shear strength s_u and the pitch p. The analytical model predicts a degree of sensitivity to the embedment depth H and helix diameter D that is not captured by the empirical model. Both models predict that the shaft diameter d has a relatively strong influence, despite a significant discrepancy arising as d becomes small. Whereas the analytical model is physically realistic as d reduces to zero, the empirical model suggests that K becomes infinite.

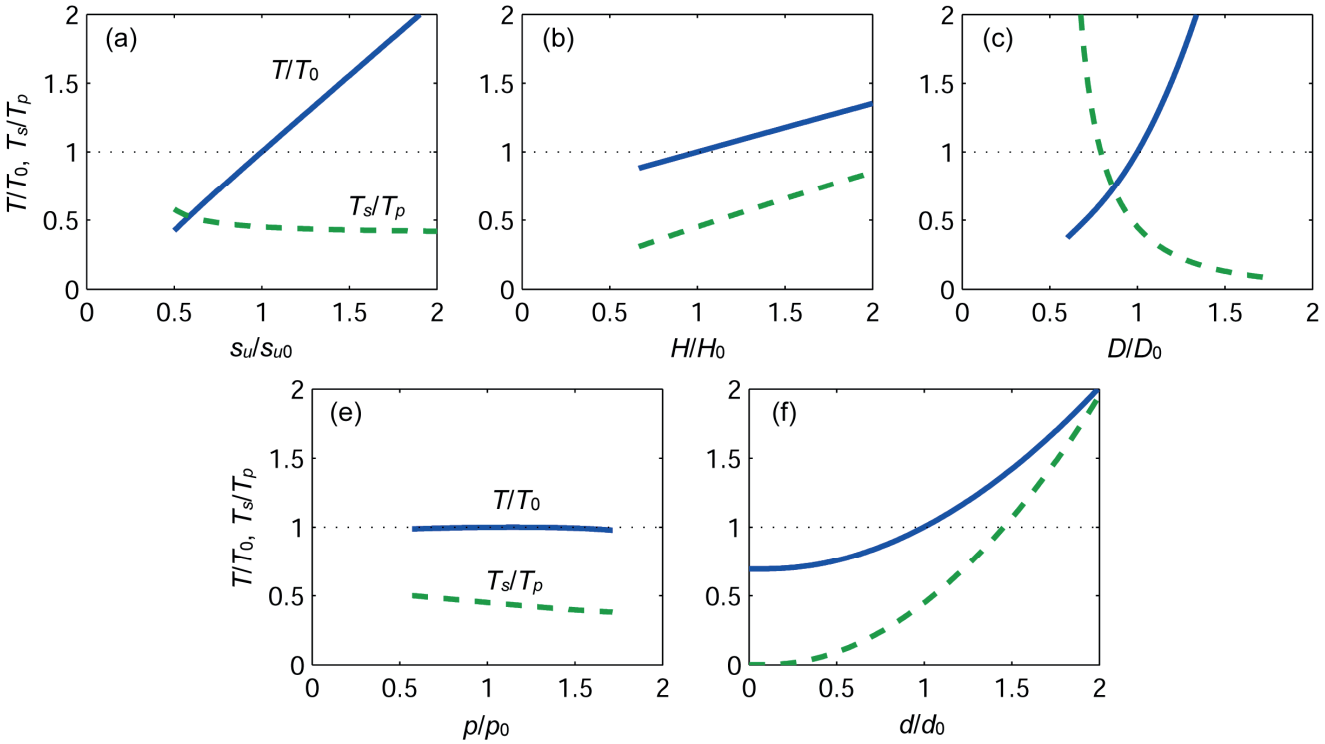

Figure 3: Variation in total installation torque T with respect to variation in undrained shear strength s_u, embedment depth H, helix diameter D, pitch p, and shaft diameter d for a fixed axial force of $N_0 = 10$ kN. Quantities are normalised by their respective base values: $T_0 = 0.69$ kN·m, $s_{u,0} = 40$ kPa, $H_0 = 1.5$ m, $D_0 = 250$ mm, $p_0 = 70$ mm, and $d_0 = 50$ mm. The dashed lines show the ratio of the torques mobilized along the shaft and the helical plate T_s/T_p.

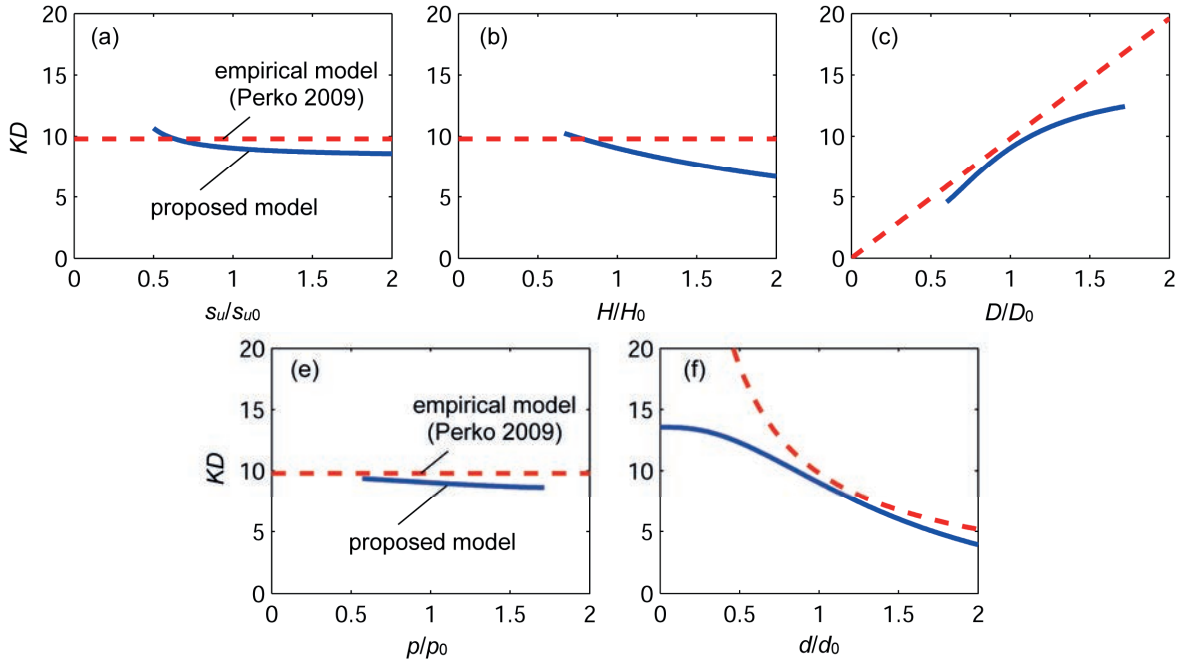

Figure 4: Variation in the normalised capacity-to-torque ratio KD with respect to variation in undrained shear strength s_u, embedment depth H, helix diameter D, pitch p, and shaft diameter d ($s_{u,0}$ = 40 kPa, H_0 = 1.5 m, D_0 = 250 mm, p_0 = 70 mm, d_0 = 50 mm, and N_0 = 10 kN). For comparison, the dashed lines show the predictions based on the empirical model given by Equation (2).

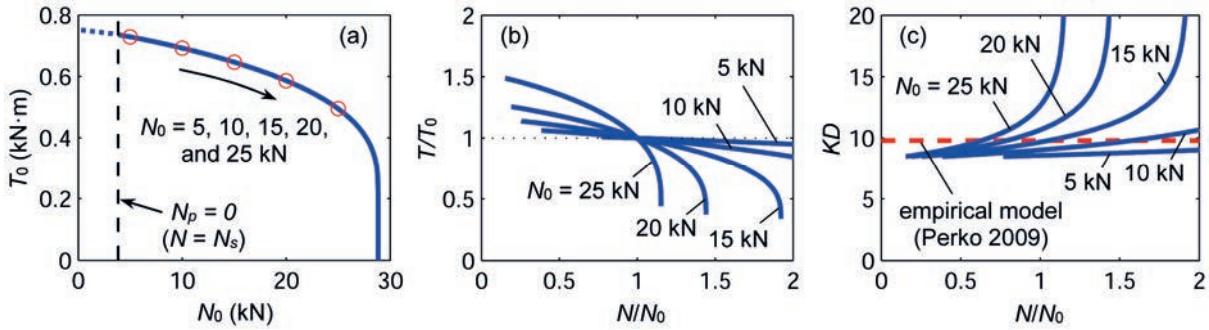

Figure 5: Variation in installation torque T and normalised capacity-to-torque ratio KD with respect to the axial force N ($s_{u,0}$ = 40 kPa, H_0 = 1.5 m, D_0 = 250 mm, p_0 = 70 mm, and d_0 = 50 mm).

Figure 5 displays the sensitivity of the intallation torque T and the normalised capacity-to-torque ratio KD to the axial force N. As shown by the yield envelope plotted in Figure 5(a), the normal force can range between 3.8 and 28.8 kN for the base parameters considered, noting that $N < N_s$ = 3.8 kN produces uplift rather than compression on the helical plate (a case not considered in this study). Figure 5(b) reveals that the installation torque T is relatively insensitive to variations in the axial force when the applied force N_0 is low (< 10 kN). However, as the applied force N_0 increases, small changes in the normal force have a pronounced influence on the torque T. The same can be said for the normalised capacity-to-torque ratio KD (Figure 5c), which displays considerable variability as the applied force N_0 increases. This behaviour can be attritubed to the shape of the yield envelope (Figure 5a), which exhibits a change in curvature from small to large values of the axial force.

4 CONCLUDING REMARKS

The paper presents a new analytical model for predicting the installation forces for deeply embedded single-helix piles in clay. The model relates the installation torque T to the soil undrained shear strength s_u, embedment depth H, helix diameter D, pitch p, shaft diameter d, and axial force N, and in combination with an approach for predicting bearing and uplift capacity, the model also furnishes predictions of the capacity-to-torque ratio often used in practice for the purpose of field verification and quality assurance. Considering a set of baseline values for the various parameters, the sensitivity analysis suggests that the installation torque T is (i) strongly dependent on the helix diameter D, undrained

shear strength s_u, and shaft diameter d, (ii) moderately dependent on embedment depth H, and (iii) virtually independent of the helix pitch p. On the other hand, the normalised capacity-to-torque ratio K is (i) strongly dependent on axial force N and the shaft diameter d, (ii) moderately dependent on the embedment depth H and helix diameter D, and (iii) largely independent of the undrained shear strength s_u and pitch p. The model provides a convenient formula that quantitatively captures the aforementioned trend and therefore represents a valuable alternative to empirical models. The analysis also reveals that the effects of the shaft are appreciable but nevertheless secondary, except in instances where the shaft diameter d is large relative to the helix diameter D.

Theoretical predictions of the capacity-to-torque ratio K based on the proposed analytical model display surprisingly good agreement with values obtained with a prevailing empirical model. The rigorous analysis completed in this study therefore lends credence to the generally accepted notion that greater difficulty in the installation of a helical pile, manifested by an increase in the installation torque T, implies a greater uplift or bearing capacity F_{max}. The sensitivity analysis suggests that caution should be exercised with respect to the applied axial force N. As N increases, the installation torque decreases, which may be advantageous, but the capacity-to-torque ratio also potentially deviates from the values predicted by the empirical model, which does not account for the axial force. The analysis illustrates that if the capacity-to-torque model is to provide reliable predictions for uplift capacity then the axial force applied during installation must be controlled and measured in addition to the installation torque.

The model proposed in this paper remains to be validated. A small-scale physical model helical pile, with torque and normal force measurements at various locations, is in development for use in the beam centrifuge at The University of Western Australia. Data from model tests performed with this apparatus will be used in the near future to assess the validity of both existing empirical models and the one proposed in this paper.

5 REFERENCES

Gaudin, C., O'Loughlin, C.D., Randolph, M.F., Cassidy, M.J., Wang, D., Tian, Y., Hambleton, J.P., Merifield, R.S. (2014). Advances in offshore and onshore anchoring solutions. *Australian Geomechanics*, 49(4), 59-72.

Ghaly, A., Hanna, A., Hanna, M. (1991). Installation torque of screw anchors in dry sand. *Soils and Foundations*, 31(2), 77-92.

Hoyt, R.M., Clemence, S.P. (1989). Uplift capacity of helical anchors in soil. *Proc. 12th International Conference on Soil Mechanics and Foundation Engineering*, 17 August, Rio de Janeiro, Brazil, Vol. 2, 1019-1022.

Martin, C.M., Randolph, M.F. (2001). Applications of the lower and upper bound theorems of plasticity to collapse of circular foundations. *Proc. 10th International Conference of the International Association for Computer Methods and Advances in Geomechanics*, 7-12 January, Tucson, USA, Vol. 2, 1417-1428.

Merifield, R.S. (2011). The ultimate uplift capacity of multi-plate helical type anchors in undrained clay. *Journal of Geotechnical and Geoenvironmental Engineering*, 137(7), 704-716.

Perko, H.A. (2009). *Helical Piles: A Practical Guide to Design and Installation*. John Wiley and Sons, Hoboken.

Perko, H.A. (2000). Energy method for predicting installation torque of helical foundations and anchors. In: Dennis, N.D., Castelli, R., O'Neill, M.W. (Eds.), *New Technological and Design Developments in Deep Foundations*, ASCE Geotechnical Special Publication No. 100, 342-352.

Todeshkejoei, C., Hambleton, J.P., Stanier, S.A., Gaudin, C. (2014). Modelling installation of helical anchors in clay. *Proc. 14th International Conference of the International Association for Computer Methods and Advances in Geomechanics*, 22-25 September, Kyoto, Japan, 917-922.

Tsuha, C.H.C, Aoki, N. (2010). Relationship between installation torque and uplift capacity of deep helical piles in sand. *Canadian Geotechnical Journal*, 47, 635-647.

Tsuha, C.H.C., Aoki, N., Rault, G., Thorel, L., Garnier, J. (2012). Evaluation of the efficiencies of helical anchor plates in sand by centrifuge model tests. *Canadian Geotechnical Journal*, 49, 1102-1114.

Wang, D., Merifield, R.S., Gaudin, C. (2013). Uplift behaviour of helical anchors in clay. *Canadian Geotechnical Journal*, 50, 575-584.